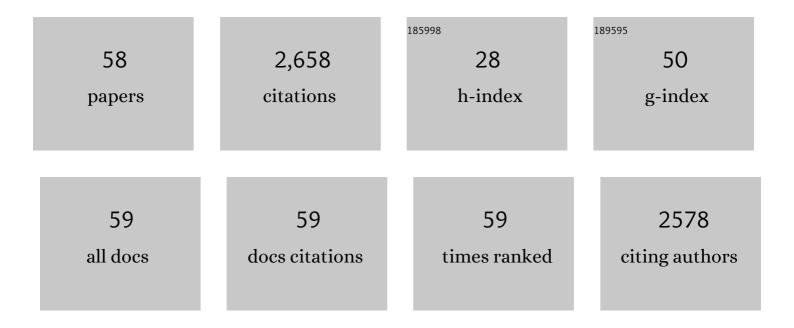
## Junie Jhon M Vequizo

List of Publications by Year in descending order

Source: https://exaly.com/author-pdf/8373321/publications.pdf Version: 2024-02-01



#	Article	IF	CITATIONS
1	Heteroatom Dopants Promote Twoâ€Electron O <sub>2</sub> Reduction for Photocatalytic Production of H <sub>2</sub> O <sub>2</sub> on Polymeric Carbon Nitride. Angewandte Chemie - International Edition, 2020, 59, 16209-16217.	7.2	270
2	Trapping-Induced Enhancement of Photocatalytic Activity on Brookite TiO <sub>2</sub> Powders: Comparison with Anatase and Rutile TiO <sub>2</sub> Powders. ACS Catalysis, 2017, 7, 2644-2651.	5.5	191
3	Distinctive Behavior of Photogenerated Electrons and Holes in Anatase and Rutile TiO <sub>2</sub> Powders. Journal of Physical Chemistry C, 2015, 119, 24538-24545.	1.5	156
4	Sequential cocatalyst decoration on BaTaO2N towards highly-active Z-scheme water splitting. Nature Communications, 2021, 12, 1005.	5.8	124
5	Curious behaviors of photogenerated electrons and holes at the defects on anatase, rutile, and brookite TiO2 powders: A review. Journal of Photochemistry and Photobiology C: Photochemistry Reviews, 2019, 40, 234-243.	5.6	113
6	Overall photosynthesis of H2O2 by an inorganic semiconductor. Nature Communications, 2022, 13, 1034.	5.8	105
7	Near infrared light induced plasmonic hot hole transfer at a nano-heterointerface. Nature Communications, 2018, 9, 2314.	5.8	103
8	Solar-driven Z-scheme water splitting using tantalum/nitrogen co-doped rutile titania nanorod as an oxygen evolution photocatalyst. Journal of Materials Chemistry A, 2017, 5, 11710-11719.	5.2	101
9	NH <sub>3</sub> -Assisted Flux Growth of Cube-like BaTaO <sub>2</sub> N Submicron Crystals in a Completely Ionized Nonaqueous High-Temperature Solution and Their Water Splitting Activity. Crystal Growth and Design, 2015, 15, 4663-4671.	1.4	95
10	Surface Modifications of (ZnSe) <sub>0.5</sub> (CuGa <sub>2.5</sub> Se <sub>4.25</sub> ) <sub>0.5</sub> to Promote Photocatalytic Z-Scheme Overall Water Splitting. Journal of the American Chemical Society, 2021, 143, 10633-10641.	6.6	88
11	Behavior and Energy State of Photogenerated Charge Carriers in Single-Crystalline and Polycrystalline Powder SrTiO <sub>3</sub> Studied by Time-Resolved Absorption Spectroscopy in the Visible to Mid-Infrared Region. Journal of Physical Chemistry C, 2015, 119, 1880-1885.	1.5	86
12	How g-C <sub>3</sub> N <sub>4</sub> Works and Is Different from TiO <sub>2</sub> as an Environmental Photocatalyst: Mechanistic View. Environmental Science & Technology, 2020, 54, 497-506.	4.6	76
13	Undoped Layered Perovskite Oxynitride Li <sub>2</sub> LaTa <sub>2</sub> O <sub>6</sub> N for Photocatalytic CO <sub>2</sub> Reduction with Visible Light. Angewandte Chemie - International Edition, 2018, 57, 8154-8158.	7.2	66
14	Simultaneously Tuning the Defects and Surface Properties of Ta <sub>3</sub> N <sub>5</sub> Nanoparticles by Mg–Zr Codoping for Significantly Accelerated Photocatalytic H <sub>2</sub> Evolution. Journal of the American Chemical Society, 2021, 143, 10059-10064.	6.6	62
15	Effects of Interfacial Electron Transfer in Metal Complex–Semiconductor Hybrid Photocatalysts on Z-Scheme CO <sub>2</sub> Reduction under Visible Light. ACS Catalysis, 2018, 8, 9744-9754.	5.5	60
16	Enhanced photocatalytic NO decomposition of visible-light responsive F-TiO2/(N,C)-TiO2 by charge transfer between F-TiO2 and (N,C)-TiO2 through their doping levels. Applied Catalysis B: Environmental, 2018, 238, 358-364.	10.8	60
17	Heteroatom Dopants Promote Twoâ€Electron O <sub>2</sub> Reduction for Photocatalytic Production of H <sub>2</sub> O <sub>2</sub> on Polymeric Carbon Nitride. Angewandte Chemie, 2020, 132, 16343-16351.	1.6	59
18	NH <sub>3</sub> -Assisted Flux-Mediated Direct Growth of LaTiO <sub>2</sub> N Crystallites for Visible-Light-Induced Water Splitting. Journal of Physical Chemistry C, 2015, 119, 15896-15904.	1.5	55

## Junie JhonÂM Vequizo

#	Article	IF	CITATIONS
19	Construction of Spatial Charge Separation Facets on BaTaO <sub>2</sub> N Crystals by Flux Growth Approach for Visible-Light-Driven H <sub>2</sub> Production. ACS Applied Materials & Interfaces, 2019, 11, 22264-22271.	4.0	51
20	Elucidating the impact of A-site cation change on photocatalytic H <sub>2</sub> and O <sub>2</sub> evolution activities of perovskite-type LnTaON <sub>2</sub> (Ln = La and Pr). Physical Chemistry Chemical Physics, 2017, 19, 22210-22220.	1.3	44
21	Copolymerization Approach to Improving Ru(II)-Complex/C <sub>3</sub> N <sub>4</sub> Hybrid Photocatalysts for Visible-Light CO <sub>2</sub> Reduction. ACS Sustainable Chemistry and Engineering, 2018, 6, 15333-15340.	3.2	40
22	Binary flux-promoted formation of trigonal ZnIn <sub>2</sub> S <sub>4</sub> layered crystals using ZnS-containing industrial waste and their photocatalytic performance for H <sub>2</sub> production. Green Chemistry, 2018, 20, 3845-3856.	4.6	38
23	Nitrogen/fluorine-codoped rutile titania as a stable oxygen-evolution photocatalyst for solar-driven Z-scheme water splitting. Sustainable Energy and Fuels, 2018, 2, 2025-2035.	2.5	36
24	Enhanced Overall Water Splitting by a Zirconiumâ€Doped TaONâ€Based Photocatalyst. Angewandte Chemie - International Edition, 2022, 61, e202116573.	7.2	36
25	Homogeneous Electron Doping into Nonstoichiometric Strontium Titanate Improves Its Photocatalytic Activity for Hydrogen and Oxygen Evolution. ACS Catalysis, 2018, 8, 7190-7200.	5.5	34
26	Clear and transparent nanocrystals for infrared-responsive carrier transfer. Nature Communications, 2019, 10, 406.	5.8	33
27	KCl flux-induced growth of isometric crystals of cadmium-containing early transition-metal (Ti 4+ ,) Tj ETQq1 1 atmosphere for water splitting application. Applied Catalysis B: Environmental, 2016, 182, 626-635.	0.784314 r 10.8	gBT /Overlock 30
28	Role of CoOx cocatalyst on Ta3N5 photocatalysts studied by transient visible to mid-infrared absorption spectroscopy. Journal of Photochemistry and Photobiology A: Chemistry, 2018, 358, 315-319.	2.0	29
29	Oxygen induced enhancement of NIR emission in brookite TiO <sub>2</sub> powders: comparison with rutile and anatase TiO <sub>2</sub> powders. Physical Chemistry Chemical Physics, 2018, 20, 3241-3248.	1.3	28
30	Core–Shell Double Doping of Zn and Ca on β-Ga <sub>2</sub> O <sub>3</sub> Photocatalysts for Remarkable Water Splitting. ACS Catalysis, 2021, 11, 1911-1919.	5.5	28
31	Improvement of photocatalytic activity under visible-light irradiation by heterojunction of Cu ion loaded WO3 and Cu ion loaded N-TiO2. Applied Catalysis B: Environmental, 2019, 248, 249-254.	10.8	27
32	The contrasting effect of the Ta/Nb ratio in (111)-layered B-site deficient hexagonal perovskite Ba <sub>5</sub> Nb <sub>4â^'x</sub> Ta <sub>x</sub> O <sub>15</sub> crystals on visible-light-induced photocatalytic water oxidation activity of their oxynitride derivatives. Dalton Transactions, 2016, 45, 12559-12568.	1.6	24
33	Identification of Individual Electron- and Hole-Transfer Kinetics at CoO <sub><i>x</i></sub> /BiVO <sub>4</sub> /SnO <sub>2</sub> Double Heterojunctions. ACS Applied Energy Materials, 2020, 3, 1207-1214.	2.5	22
34	Crucial impact of reduction on the photocarrier dynamics of SrTiO <sub>3</sub> powders studied by transient absorption spectroscopy. Journal of Materials Chemistry A, 2019, 7, 26139-26146.	5.2	21
35	Efficient photocatalytic hydrogen evolution on single-crystalline metal selenide particles with suitable cocatalysts. Chemical Science, 2020, 11, 6436-6441.	3.7	21
36	Enhanced Visible Light Response of TiO <sub>2</sub> Codoped with Cr and Ta Photocatalysts by Electron Doping. ACS Applied Energy Materials, 2019, 2, 3274-3282.	2.5	20

Junie JhonÂM Vequizo

#	Article	IF	CITATIONS
37	Enhancement of photoelectrochemical activity of SnS thin-film photoelectrodes using TiO2, Nb2O5, and Ta2O5metal oxide layers. Applied Physics Express, 2016, 9, 067101.	1.1	18
38	Fabrication of robust TiO2 thin films by atomized spray pyrolysis deposition for photoelectrochemical water oxidation. Journal of Photochemistry and Photobiology A: Chemistry, 2018, 358, 320-326.	2.0	17
39	Undoped Layered Perovskite Oxynitride Li <sub>2</sub> LaTa <sub>2</sub> O <sub>6</sub> N for Photocatalytic CO <sub>2</sub> Reduction with Visible Light. Angewandte Chemie, 2018, 130, 8286-8290.	1.6	17
40	Electrodeposition of SnO <sub>2</sub> Thin Films from Aqueous Tin Sulfate Solutions. Japanese Journal of Applied Physics, 2010, 49, 125502.	0.8	16
41	Fabrication of Electrodeposited SnS/SnO <sub>2</sub> Heterojunction Solar Cells. Japanese Journal of Applied Physics, 2012, 51, 10NC38.	0.8	16
42	Cocatalyst engineering of a narrow bandgap Ga-La <sub>5</sub> Ti <sub>2</sub> Cu <sub>0.9</sub> Ag <sub>0.1</sub> O <sub>7</sub> S <sub>5</sub> photocatalyst towards effectively enhanced water splitting. Journal of Materials Chemistry A, 2021, 9, 27485-27492.	5.2	16
43	Enhanced water splitting through two-step photoexcitation by sunlight using tantalum/nitrogen-codoped rutile titania as a water oxidation photocatalyst. Sustainable Energy and Fuels, 2019, 3, 2337-2346.	2.5	14
44	Expansion of the photoresponse window of a BiVO <sub>4</sub> photocatalyst by doping with chromium( <scp>vi</scp> ). RSC Advances, 2018, 8, 38140-38145.	1.7	13
45	A Na-containing Pt cocatalyst for efficient visible-light-induced hydrogen evolution on BaTaO <sub>2</sub> N. Journal of Materials Chemistry A, 2021, 9, 13851-13854.	5.2	13
46	Electrodeposition and Characterization of $\hat{I}^3$ -FeOOH Thin Films from Oxygen-Bubbled Aqueous Iron Sulfate Solutions. Applied Physics Express, 2013, 6, 125501.	1.1	12
47	Effect of CuFe2O4 ferrite on photocatalysis and carrier dynamics of electrospun α-Fe2O3 nanofibers by time-resolved transient absorption spectroscopy. Ceramics International, 2019, 45, 15676-15680.	2.3	12
48	Fe/Ru Oxide as a Versatile and Effective Cocatalyst for Boosting Z-Scheme Water-Splitting: Suppressing Undesirable Backward Electron Transfer. ACS Applied Materials & Interfaces, 2019, 11, 45606-45611.	4.0	11
49	Oxygenâ€Doped Ta <sub>3</sub> N <sub>5</sub> Nanoparticles for Enhanced Zâ€6cheme Carbon Dioxide Reduction with a Binuclear Ruthenium(II) Complex under Visible Light. ChemPhotoChem, 2019, 3, 1027-1033.	1.5	10
50	Fabrication of Electrodeposited SnS/SnO <sub>2</sub> Heterojunction Solar Cells. Japanese Journal of Applied Physics, 2012, 51, 10NC38.	0.8	10
51	Fabrication of Cu <sub>2</sub> 0/γ-FeOOH heterojunction solar cells using electrodeposition. Applied Physics Express, 2014, 7, 045501.	1.1	9
52	Sodium titanium oxide bronze nanoparticles synthesized <i>via</i> concurrent reduction and Na <sup>+</sup> -doping into TiO <sub>2</sub> (B). Nanoscale, 2019, 11, 1442-1450.	2.8	8
53	Electrodeposition of Ga–O Thin Films from Aqueous Gallium Sulfate Solutions. Japanese Journal of Applied Physics, 2013, 52, 075503.	0.8	3
54	Influences of pulverization and annealing treatment on the photocatalytic activity of BiVO <sub>4</sub> for oxygen evolution. Sustainable Energy and Fuels, 2022, 6, 1698-1707.	2.5	3

#	Article	IF	CITATIONS
55	Enhanced Overall Water Splitting by a Zirconiumâ€Đoped TaONâ€Based Photocatalyst. Angewandte Chemie, 2022, 134, .	1.6	2
56	Modified SILAR Grown ZnO Films on <i>p</i> ‣i(100) with Enhanced Charge Separation for UV Light Sensing Application. Physica Status Solidi (A) Applications and Materials Science, 2021, 218, 2100363.	0.8	1
57	An equation of average lifetime of the minority carriers in semiconductors from photo-electrochemical measurement. Transactions of the Materials Research Society of Japan, 2013, 38, 385-388.	0.2	1
58	Annealing Effect of the Cu <sub>x</sub> O Thin Films Prepared by Drop Chemical Technique. Transactions of the Materials Research Society of Japan, 2014, 39, 109-112.	0.2	1